THE JOURNAL OF PHYSICAL CHEMISTRY LETTERS
A JOURNAL OF THE AMERICAN CHEMICAL SOCIETY

pubs.acs.org/JPCL

Letter

Unraveling the Contribution of Residual Monomer to the Emission Spectra of Poly(3-hexylthiophene) Aggregates: Implications for Identifying H- and J-type Coupling

Stephanie N. Kramer, Jasper Brown, Megan Rice, and Linda A. Peteanu*

Cite This: J. Phys. Chem. Lett. 2021, 12, 5919–5924

Read Online

ACCESS | Metrics & More | Article Recommendations | Supporting Information

ABSTRACT: Poly(3-hexylthiophene) (P3HT) is a well-studied benchmark system for semiconducting polymers used in optoelectronic devices. In these materials, aggregation can improve charge transport efficiency or enhance emission yields depending on the interchain packing. This may be inferred from the absorption and emission spectra when analyzed using exciton coupling models such as the well-known H- and J-coupling model of Kasha. The more recently developed weakly coupled H-aggregate (WCH) model quantifies the degree of disorder via the ratio of the electronic origin intensity to that of the first vibronic band. Here, the underlying assumptions of this approach are tested experimentally for P3HT aggregates formed by solvent poisoning using bulk and single-molecule-based spectroscopic techniques. Specifically, we show that the contribution of residual monomeric chains to the aggregate spectrum must be accounted for to properly assign the spectra as H- or J-type. A modification of the WCH model is introduced to account for multiple emissive species.

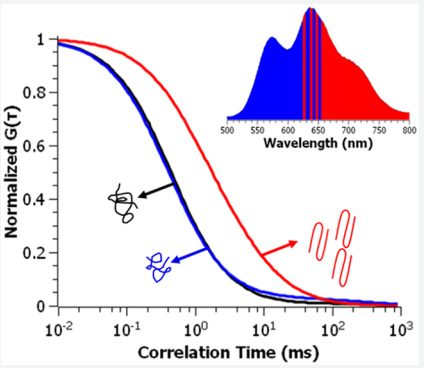

In the optoelectronics field, regioregular poly(3-hexylthiophene) (rr-P3HT, Chart 1) is a benchmark polymer that

Chart 1. Structure of rr-P3HT

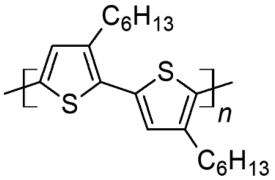

has been incorporated into devices such as transistors[1−3] and photovoltaics.[4−6] As is the case for most conjugated polymers, rr-P3HT will aggregate in a highly concentrated solution or in the solid state if nothing preemptive is done such as filtering the solution or diluting the polymer into a host matrix.[7,8] The standard means of determining the degree of aggregation and the type of chain packing is via analysis of absorption/emission spectra derived from the well-known model of small-molecule aggregation of Kasha.[9]

Within the excitonic coupling model, coupling between the transition moments of molecules in close proximity (i.e., aggregated) causes a splitting of the energy levels corresponding to the in-phase and out-of-phase linear combinations. When the in-phase combination is lower in energy, the aggregate is referred to as J-type, while if the out-of-phase combination is lowest, the aggregate is H-type. rr-P3HT and other conjugated polymers are considered to form weakly coupled H-aggregates under most common conditions.[7,10−14] Their absorption and emission spectra are weakly red-shifted from that of the corresponding monomer due to the planarized chain morphology.[15] Interestingly, while H-type aggregation predominates in P3HT, conditions have been found that produce predominantly J-type, suggesting that the aggregate type can be controlled by the processing conditions.[14,16,17]

Spano and coauthors[10,15,18] have elaborated this basic Kasha model to account for the evolution of spectral features for cases in which the excitonic coupling is weak but H-type in nature (weakly coupled H-aggregate, WCH), as this is the predominant mode seen in numerous conjugated materials. We focus here on how the WCH model is used to assess the degree of aggregate disorder by analyzing the Franck−Condon envelope of the aggregate absorption and emission spectra.[15,18] Briefly, in a well-ordered H-aggregate, the electronic origin (0−0 band) is formally forbidden due to the cancellation of transition moments whereas the vibronic bands (the 0−1 and 0−2 transitions) may still be observed. In most conjugated materials, these bands will correspond to the C═C stretch. The result is a vibronic envelope that is distinct from that of the monomer. Disorder within the aggregate can cause this selection rule to break down, resulting in a nonzero intensity in

Received: April 23, 2021
Accepted: June 17, 2021
Published: June 22, 2021

https://doi.org/10.1021/acs.jpclett.1c01334
J. Phys. Chem. Lett. 2021, 12, 5919−5924

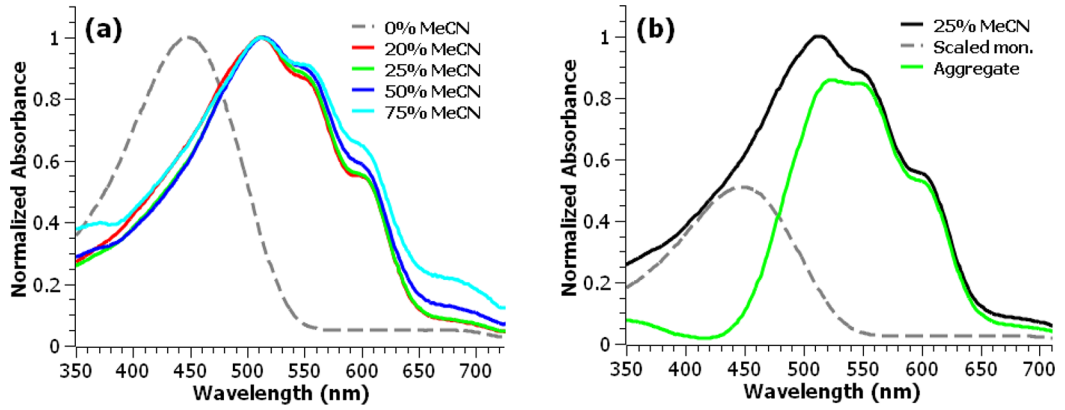

Figure 1. (a) Normalized absorption spectra of nonaggregated and preaggregated rr-P3HT/THF samples and (b) absorption spectra of aggregated rr-P3HT/THF in 25% MeCN with the absorption of nonaggregated rr-P3HT/THF subtracted. The resulting spectrum is that of the aggregate species.

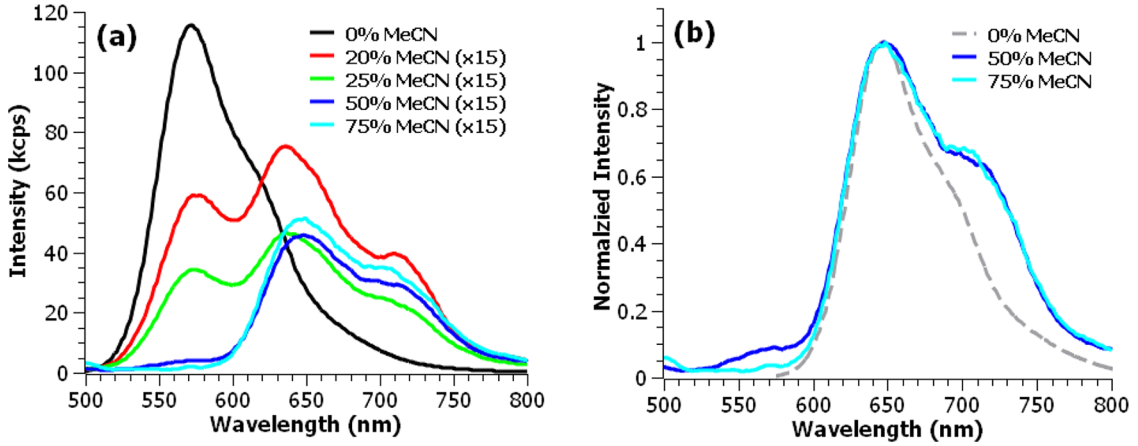

Figure 2. (a) Emission spectra (scaled to absorbance at 485 nm) of nonaggregated and preaggregated rr-P3HT/THF samples and (b) overlay of the emission bands of the nonaggregated and preaggregated rr-P3HT in 50% and 75% MeCN. The monomer spectrum is shifted 75 nm to lower energies to overlap with that of the 50% and 75% aggregate spectra.

the 0−0 band. To quantify the degree of disorder in H-aggregates, the intensity ratio of the electronic origin to the first vibronic band is commonly quoted.[10] More recently, this model has been expanded to account for the ability of the same molecule to adopt H- versus J-type electronic coupling due to the ability of the local environment to influence the packing of the chains (HJ coupling model).[18−20]

The WCH model has provided a fruitful way of interpreting the unusual band shapes of P3HT and other conjugated materials in aggregated or thin film form.[7,10−14] One potential complication, however, stems from the underlying assumption that the bulk spectrum corresponds to a single species (monomer or aggregate) to which all the spectral features can be attributed. Here we demonstrate how this assumption can be tested using fluorescence-based methods and under which conditions it is found lacking, particularly in the analysis of conjugated polymers aggregated in solution using a solvent poisoning method. The implications for interpreting aggregate morphological properties using linear absorption and emission spectra are then discussed.

In tetrahydrofuran (THF), rr-P3HT is not aggregated and exhibits a broad absorption feature at 450 nm whereas addition of poor solvent such as acetonitrile (MeCN) results in a spectrum with enhanced vibrational structure shifted by 150 nm to lower energies (Figure 1a).

Following the analysis of Clark et al.,[11] subtracting the monomer (i.e., unaggregated chain) spectrum from that of the preaggregated samples reveals the presence of two absorptive species in all preaggregated samples (Figure 1b and Figure S1, Supporting Information). The resulting aggregate spectrum is very similar to that obtained by Clark et al. in thin films cast from chloroform, and a similar approach is used here to fit the data to extract the Huang−Rhys factor (S) and exciton bandwidth (W) of the aggregate (Supporting Information Section S2).[11] There, the results of various fitting approaches are compared including using the S values determined via fitting the emission spectra (see below) and literature values for both S[21] and W.[11] That there is a significant percentage of unaggregated chains, even at high concentrations of MeCN, is somewhat surprising and important for the analysis of the emission spectra that follows.

The emission of rr-P3HT in THF (Figure 2a) is also indicative of an unaggregated solution with a strong 0−0 transition at 570 nm and smaller 0−1 sideband at 620 nm.[11,13] On addition of MeCN, the vibronic structure is perturbed and the emission is strongly quenched. At lower percentages of MeCN (20−25%), the spectra are very similar to those reported previously for the polymer in thin films and assigned as weakly coupled H-aggregates.[11,13,22,23] Interestingly, simply increasing the percentage of MeCN produces aggregates with

https://doi.org/10.1021/acs.jpclett.1c01334
J. Phys. Chem. Lett. 2021, 12, 5919−5924

spectra very similar to those reported for highly ordered P3HT nanofibers that have been assigned as J-aggregates.[16,24,25]

Results similar to those in Figure 2 have been previously reported in P3HT[11,13,26−29] and several other organic conjugated systems[12,17,30,31] and were ascribed to evolution of the most favorable aggregate structure from H-like to J-like due to solvent-induced forces. Changing pressure or temperature produces similar effects that have been attributed to alterations in the chain packing and therefore the electronic coupling between the chains.[16,24,25] Next, we examine various existing models to fit the rr-P3HT emission spectra and to explain its evolution with increasing poor solvent and then describe experiments that support an alternative approach.

One way to model the emission spectra is to assume the S value of the C═C vibronic mode increases with decreasing solvent quality. In this case, the spectra are considered to derive from a single emitter type and are fit using eq 1 by assigning the band at 570 nm as the 0−0 band of the aggregate and 650 nm as the 0−1 of the C═C stretching mode.[32]

$$\frac{I_{0-m}}{I_{0-n}} \propto \frac{(\hbar\omega_m)^3 S^m n!}{(\hbar\omega_n)^3 S^n m!} \tag{1}$$

Here, I is the emission peak intensities of the transition band determined experimentally, m and n are the quantum numbers of the final states of the transitions, and $\hbar\omega$ is the transition energy.

Below 50% MeCN, the apparent S values determined by eq 1 increase from that of the monomer ($S \sim 1$) to ∼1.8 for the 25% MeCN sample, which would be indicative of an increase in geometric distortion in the aggregated chains. However, at 50% MeCN and above, the effective disappearance of the 570 nm band would lead to unphysically large Huang−Rhys factors ($S > 10$) within this model. Alternatively, the spectrum at high MeCN percentages is plausibly assigned to an aggregate with 0−0 and 0−1 transitions at 650 and 720 nm, respectively. Notably, the vibronic structure of these aggregates (Figure 2b) is similar to that of the monomer albeit red-shifted 80 nm. This assignment yields in an S value of 0.88 (eq 1). As neither the spectral shape nor the intensity changes with additional MeCN, this likely represents the fully aggregated species. Proposed interpretations of this spectrum are deferred to a later section.

Next, we consider the WCH model, described earlier, that has been frequently applied to P3HT.[7,10−13,17,33] In this fitting approach (eq 2) the 0−0 band intensity is varied independently while the vibronic transitions are fit using the expected Franck−Condon intensity distribution assuming a single S for the C═C mode.

$$\frac{P(\hbar\omega)}{n^3(\hbar\omega)^3} \sim \alpha\Gamma(\hbar\omega - E_0) + \sum_{m=1} \frac{S^m}{m!}\Gamma\delta[\hbar\omega - (E_0 - mE_d)] \tag{2}$$

Here, n is the refractive index, $\hbar\omega$ is the photon energy, α is a scaling factor that is allowed to vary, Γ is the Gaussian line width function, E_0 is the 0−0 transition energy, and E_d is the energy of the C═C vibrational mode (set to 0.175 eV).[13] The S values of these systems were determined via a nonlinear least-squares fit of eq 2. The resulting S values using the WCH model for the 20% and 25% MeCN samples are identical (1.14) and only slightly higher than that of the monomer ($S_{0\%}$ = 1.11), whereas those for higher percentages of MeCN are larger (1.18).

More recently, the WCH model has been expanded[20] to explain the type of spectral evolution seen in Figure 2a that is commonly seen in conjugated organics with decreasing solvent quality or changes in temperature or pressure.[12,16,30,34−36] This has been ascribed to a change from H- to J-type packing driven by the environment.[14,16,17,24,25] Therefore, these systems are referred to as HJ-aggregates as their spectral properties are governed by the relative magnitudes of the H- and J-type coupling. Applying this model to our results, the spectra at 50% MeCN and above would be assigned to a J-aggregate whereas all the vibronic features of the aggregate at lower MeCN percentages would be ascribed to the H-aggregate form.

The two models discussed thus far implicitly assume that the aggregates formed at a given MeCN percentage are of a single type, meaning they all have similar spectra, mode frequencies, S values, electronic couplings, and degree of chain ordering. Though this approach provides reasonably high-quality fits to the vibronic structure of the bulk solution emission spectra (Figure S4), it is at odds with several experimental results described next. Specifically, we show evidence that the apparent spectral evolution from the H-type to J-type coupling seen in Figure 2a is in fact due to decreasing contributions from monomeric chains as the solvent quality declines.

Fluorescence excitation spectroscopy is a convenient means of determining whether a bulk sample consists of a single or multiple emitting species with distinct absorption spectra. At less than 50% MeCN, the peak of the emission spectrum is dependent on the excitation wavelength used (Figure S5) and therefore shows two peaks, one at 570 nm and one at 650 nm. In contrast, at greater than 50% MeCN, ,a single peak at 650 nm is observed. Comparison of the excitation spectra at 570 and 650 nm with the monomer and aggregate absorption spectra (Supporting Information Section S5) shows the gradual appearance of two emitting species with increasing MeCN whereas only one is present in the monomer solution, as expected.

Strong supporting evidence for assigning the spectra (Figure 2a) to the coexistence of monomer and aggregated chains is obtained via fluorescence correlation spectroscopy (FCS). In solution, FCS can be used to determine the degree of polymer aggregation by measuring fluctuations in the emission intensity as each species diffuses through the focal volume.[8] In general, if an emission spectrum arises from a single species, then collecting the FCS at various wavelengths within the spectrum will yield identical correlation curves and diffusion times (τ_D). This is the case for the monomer when FCS curves are collected at 540 and 700 nm (data not shown). In contrast, if the FCS curve differs with collection wavelength, the presence of more than one species having both different emission maxima and diffusion rates can be inferred. As a practical matter, two species can be differentiated by FCS if the difference in the mass is at least a factor of 4, which would be consistent with the formation of intermolecular (multichain) aggregates.[37,38] Comparing the normalized FCS curves (Figure 3) clearly shows that the diffusion rate for the 540 nm emitting species in 25% MeCN (0.61 ± 0.10 ms) is similar to that of the monomer in THF (0.54 ± 0.02 ms) whereas that collected at 700 nm is significantly longer (3.1 ± 0.9 ms). This longer diffusion time indicates a larger emitter (estimated to be ∼100 nm in size compared to ∼20 nm for the monomer), which is consistent with aggregation and qualitatively supported by

https://doi.org/10.1021/acs.jpclett.1c01334
J. Phys. Chem. Lett. 2021, 12, 5919−5924

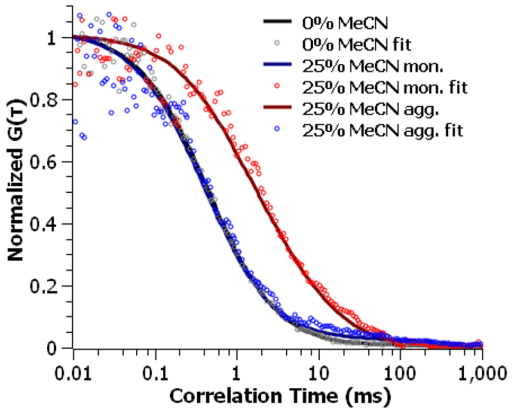

Figure 3. Normalized FCS decay curves of nonaggregated and 25% MeCN preaggregated rr-P3HT/THF samples. Optical filters were chosen to selectively measure the fluorescence bursts of the monomer and aggregate species.

dynamic light scattering (DLS) measurements (Figure S8).[8,37,38] At higher percentages of MeCN, the signal could not be distinguished from background.

These experimental results suggest an alternate approach to fitting the spectra at low MeCN percentages, which is to assume that they arise from a heterogeneous mixture of monomeric and aggregated chains as is the case in absorption (Figure 1b). In this multiemitting species model (MES), the ratio of monomers to aggregates decreases as the quality of the solvent environment declines. Here, the fitting to eq 2 is modified from that of the WCH model to account for the presence of residual monomer (eq 3).

$$\frac{P(\hbar\omega)}{n^3(\hbar\omega)^3} \sim \left(\alpha_{\mathrm{mon}} \sum_{m=0} \frac{S_{\mathrm{mon}}^m}{m!} \Gamma\delta[\hbar\omega - (E_0 - mE_{\mathrm{d}})]\right) + \left(\alpha\Gamma(\hbar\omega - E_0) + \sum_{m=1} \frac{S^m}{m!} \Gamma\delta[\hbar\omega - (E_0 - mE_{\mathrm{d}})]\right) \quad (3)$$

The fit is performed accounting for the 0−0, 0−1, and 0−2 of the monomer in addition to assuming the band at 650 nm to be the electronic origin of the aggregate. The percentage of monomer is allowed to vary independently and should decrease in its contribution the more aggregated the sample. The MES model results in an overall decrease in the Huang−Rhys factors to nearly 1 for all conditions ($S_{20\%}^{\mathrm{MES}}$ = 1.02, $S_{25\%}^{\mathrm{MES}}$ = 1.03, $S_{50\%}^{\mathrm{MES}}$ = 1.01, $S_{75\%}^{\mathrm{MES}}$ = 1.01) and a slightly better fit to the experimental data (R^2 = 0.99, Figure 4 and Figure S9) as compared to the WCH model (R^2 = 0.97, Figure S4).

Consistent with the MES model, subtracting the spectrum of the monomer from the low percentages of MeCN (Figure S10) resulted in a spectrum nearly identical to that of the aggregate (50% and 75% MeCN, Figure S11) and a decrease in the S values ($S_{20\%\mathrm{sub}}^{\mathrm{MES}}$ = 1.00 and $S_{25\%\mathrm{sub}}^{\mathrm{MES}}$ = 1.02).

In summary, though the MES gives a somewhat better fit to the data than does the WCH model, as judged by the R^2 values, this does not in itself establish its validity. Rather, this is strongly suggested from the experimental evidence that emission from monomeric chains contributes substantially to the observed vibronic envelope of the aggregates, particularly at lower MeCN percentages.

Within this picture, the evolution of the emission spectra with decreasing solvent quality (Figure 2a) results from a decrease in the percentage of monomer present and the emergence of an aggregate species with an electronic origin at 650 nm and a J-like vibronic structure. In contrast, the HJ model would attribute this spectral evolution to a change from a weakly coupled H-aggregate to a J-aggregate with the change in solvent quality.[16,17,24,25]

Notably, the aggregate spectra of Figure 2b are similar to those reported for J-type P3HT nanofibers in both peak positions and relative vibronic intensities. However, neither these J-type aggregates nor those reported[16,24,39] exhibit the classical behavior of spectral narrowing,[40] reduced vibronic band intensity, and decreased lifetime[41,42] relative to the monomer. This may indicate some degree of chain disorder that diminishes their electronic coherence. If the aggregates formed under our conditions are indeed J-type, their weak emission intensity relative to the monomer is unexpected (Figure 2a). However, the emission lifetimes in solution are slightly decreased relative to the monomer (Figure S12 and Table S5) within our time resolution of ∼200 ps, which is expected for J-aggregates.[43,44] Notably, there is a greater loss of emission intensity upon aggregation (approximately a factor of 35; see Figure 2a) than what would be predicted from the decrease in lifetime relative to the monomer (Table S5). This apparent discrepancy suggests a static quenching mechanism contributes to the emission loss upon aggregation, i.e., that a subpopulation of nonemissive species is present. We hypothesize that these represent a subpopulation of nonemissive H-aggregates formed under our conditions. Alternate mechanisms for emission quenching such as solvent-polarity-

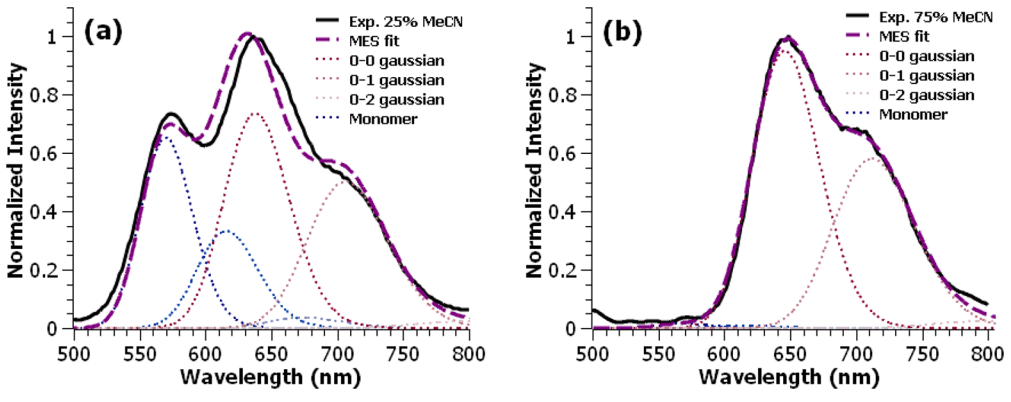

Figure 4. Fits of the MES model to the experimental data for rr-P3HT/THF in (a) 25% and (b) 75% MeCN.

https://doi.org/10.1021/acs.jpclett.1c01334
J. Phys. Chem. Lett. 2021, 12, 5919−5924

induced stabilization of a dark charge-transfer state[31,45] or polaron pair formation[46,47] are also possible and will be explored further in a future communication.

Using the tools of fluorescence excitation spectroscopy and FCS, we have shown that the apparent evolution of the emission spectrum of rr-P3HT from weakly coupled H-like to J-like with decreasing solvent quality can instead be explained by an accompanying decrease in the percentage of residual monomer. Consistent with this picture, high-quality fits of the emission spectra at various percentages of poor solvent are obtained using a model that allows the percent of aggregate and monomer to vary independently. The applicability of this approach to other conjugated systems is a target of future exploration.

■ ASSOCIATED CONTENT

Supporting Information

The Supporting Information is available free of charge at https://pubs.acs.org/doi/10.1021/acs.jpclett.1c01334.

Description of absorption modeling method, model fits, subtracted absorption and emission spectra, emission maps, excitation spectra, DLS histograms, lifetime decays, Huang−Rhys factors, and experimental methods (PDF)

■ AUTHOR INFORMATION

Corresponding Author

Linda A. Peteanu − *Department of Chemistry, Carnegie Mellon University, Pittsburgh, Pennsylvania 15213, United States;* orcid.org/0000-0003-0075-6521; Email: peteanu@cmu.edu

Authors

Stephanie N. Kramer − *Department of Chemistry, Carnegie Mellon University, Pittsburgh, Pennsylvania 15213, United States;* orcid.org/0000-0003-1650-6834

Jasper Brown − *Department of Chemistry, Carnegie Mellon University, Pittsburgh, Pennsylvania 15213, United States;* Present Address: Department of Chemistry, University of Chicago, 5801 S. Ellis Ave., Chicago, Illinois 60637, United States.

Megan Rice − *Department of Chemistry, Carnegie Mellon University, Pittsburgh, Pennsylvania 15213, United States*

Complete contact information is available at: https://pubs.acs.org/10.1021/acs.jpclett.1c01334

Notes

The authors declare no competing financial interest.

■ ACKNOWLEDGMENTS

The authors acknowledge the financial support of the NSF through CHE-1900506. We also thank Matthew Baker, Michael Bautista, and Kevin Noonan (CMU) for synthesis of the P3HT used here.

■ REFERENCES

(1) Sirringhaus, H.; Brown, P. J.; Friend, R. H.; Nielsen, M. M.; Bechgaard, K.; Langeveld-Voss, B. M. W.; Spiering, A. J. H.; Janssen, R. a. J.; Meijer, E. W.; Herwig, P.; de Leeuw, D. M. Two-Dimensional Charge Transport in Self-Organized, High-Mobility Conjugated Polymers. *Nature* **1999**, *401*, 685−688.

(2) Zen, A.; Pflaum, J.; Hirschmann, S.; Zhuang, W.; Jaiser, F.; Asawapirom, U.; Rabe, J. P.; Scherf, U.; Neher, D. Effect of Molecular Weight and Annealing of Poly(3-hexylthiophene)s on the Performance of Organic Field-Effect Transistors. *Adv. Funct. Mater.* **2004**, *14*, 757−764.

(3) Yang, H.; Shin, T. J.; Yang, L.; Cho, K.; Ryu, C. Y.; Bao, Z. Effect of Mesoscale Crystalline Structure on the Field-Effect Mobility of Regioregular Poly(3-Hexyl Thiophene) in Thin-Film Transistors. *Adv. Funct. Mater.* **2005**, *15*, 671−676.

(4) Yu, G.; Gao, J.; Hummelen, J. C.; Wudl, F.; Heeger, A. J. Polymer Photovoltaic Cells: Enhanced Efficiencies via a Network of Internal Donor-Acceptor Heterojunctions. *Science* **1995**, *270*, 1789−1791.

(5) Brabec, C. J.; Sariciftci, N. S.; Hummelen, J. C. Plastic Solar Cells. *Adv. Funct. Mater.* **2001**, *11*, 15−26.

(6) Kim, Y.; Cook, S.; Tuladhar, S. M.; Choulis, S. A.; Nelson, J.; Durrant, J. R.; Bradley, D. D. C.; Giles, M.; McCulloch, I.; Ha, C.-S.; Ree, M. A Strong Regioregularity Effect in Self-Organizing Conjugated Polymer Films and High-Efficiency Polythiophene:Fullerene Solar Cells. *Nat. Mater.* **2006**, *5*, 197−203.

(7) Thiessen, A.; Vogelsang, J.; Adachi, T.; Steiner, F.; Bout, D. V.; Lupton, J. M. Unraveling the Chromophoric Disorder of Poly(3-Hexylthiophene). *Proc. Natl. Acad. Sci. U. S. A.* **2013**, *110*, E3550−E3556.

(8) Wu, E. C.; Stubbs, R. E.; Peteanu, L. A.; Jemison, R.; McCullough, R. D.; Wildeman, J. Detection of Ultralow Concentrations of Non-Emissive Conjugated Polymer Aggregates via Fluorescence Correlation Spectroscopy. *J. Phys. Chem. B* **2017**, *121*, 5413−5421.

(9) Kasha, M. Energy Transfer Mechanisms and the Molecular Exciton Model for Molecular Aggregates. *Radiat. Res.* **1963**, *20*, 55−70.

(10) Spano, F. C. Modeling Disorder in Polymer Aggregates: The Optical Spectroscopy of Regioregular Poly(3-Hexylthiophene) Thin Films. *J. Chem. Phys.* **2005**, *122*, 234701.

(11) Clark, J.; Silva, C.; Friend, R. H.; Spano, F. C. Role of Intermolecular Coupling in the Photophysics of Disordered Organic Semiconductors: Aggregate Emission in Regioregular Polythiophene. *Phys. Rev. Lett.* **2007**, *98*, 206406.

(12) Brazard, J.; Ono, R. J.; Bielawski, C. W.; Barbara, P. F.; Vanden Bout, D. A. Mimicking Conjugated Polymer Thin-Film Photophysics with a Well-Defined Triblock Copolymer in Solution. *J. Phys. Chem. B* **2013**, *117*, 4170−4176.

(13) Panzer, F.; Sommer, M.; Bässler, H.; Thelakkat, M.; Köhler, A. Spectroscopic Signature of Two Distinct H-Aggregate Species in Poly(3-Hexylthiophene). *Macromolecules* **2015**, *48*, 1543−1553.

(14) Eder, T.; Stangl, T.; Gmelch, M.; Remmerssen, K.; Laux, D.; Höger, S.; Lupton, J. M.; Vogelsang, J. Switching between H- and J-Type Electronic Coupling in Single Conjugated Polymer Aggregates. *Nat. Commun.* **2017**, *8*, 1641.

(15) Spano, F. C.; Silva, C. H- and J-Aggregate Behavior in Polymeric Semiconductors. *Annu. Rev. Phys. Chem.* **2014**, *65*, 477−500.

(16) Niles, E. T.; Roehling, J. D.; Yamagata, H.; Wise, A. J.; Spano, F. C.; Moulé, A. J.; Grey, J. K. J-Aggregate Behavior in Poly-3-Hexylthiophene Nanofibers. *J. Phys. Chem. Lett.* **2012**, *3*, 259−263.

(17) Marques, S. R.; Labastide, J. A.; Barnes, M. D. Evolution of HJ Coupling in Nanoscale Molecular Self-Assemblies. *J. Phys. Chem. C* **2018**, *122*, 15723−15728.

(18) Hestand, N. J.; Spano, F. C. Molecular Aggregate Photophysics beyond the Kasha Model: Novel Design Principles for Organic Materials. *Acc. Chem. Res.* **2017**, *50*, 341−350.

(19) Spano, F. C. The Spectral Signatures of Frenkel Polarons in H- and J-Aggregates. *Acc. Chem. Res.* **2010**, *43*, 429−439.

(20) Yamagata, H.; Spano, F. C. Interplay between Intrachain and Interchain Interactions in Semiconducting Polymer Assemblies: The HJ-Aggregate Model. *J. Chem. Phys.* **2012**, *136*, 184901.

(21) Clark, J.; Chang, J.-F.; Spano, F. C.; Friend, R. H.; Silva, C. Determining Exciton Bandwidth and Film Microstructure in Polythiophene Films Using Linear Absorption Spectroscopy. *Appl. Phys. Lett.* **2009**, *94*, 163306.

(22) Brown, P. J.; Thomas, D. S.; Köhler, A.; Wilson, J. S.; Kim, J.-S.; Ramsdale, C. M.; Sirringhaus, H.; Friend, R. H. Effect of Interchain Interactions on the Absorption and Emission of Poly(3-Hexylthiophene). *Phys. Rev. B: Condens. Matter Mater. Phys.* **2003**, *67*, No. 064203.
(23) Panzer, F.; Bässler, H.; Lohwasser, R.; Thelakkat, M.; Köhler, A. The Impact of Polydispersity and Molecular Weight on the Order−Disorder Transition in Poly(3-Hexylthiophene). *J. Phys. Chem. Lett.* **2014**, *5*, 2742−2747.
(24) Martin, T. P.; Wise, A. J.; Busby, E.; Gao, J.; Roehling, J. D.; Ford, M. J.; Larsen, D. S.; Moulé, A. J.; Grey, J. K. Packing Dependent Electronic Coupling in Single Poly(3-Hexylthiophene) H- and J-Aggregate Nanofibers. *J. Phys. Chem. B* **2013**, *117*, 4478−4487.
(25) Baghgar, M.; Labastide, J. A.; Bokel, F.; Hayward, R. C.; Barnes, M. D. Effect of Polymer Chain Folding on the Transition from H- to J-Aggregate Behavior in P3HT Nanofibers. *J. Phys. Chem. C* **2014**, *118*, 2229−2235.
(26) Chen, P.-Y.; Rassamesard, A.; Chen, H.-L.; Chen, S.-A. Conformation and Fluorescence Property of Poly(3-Hexylthiophene) Isolated Chains Studied by Single Molecule Spectroscopy: Effects of Solvent Quality and Regioregularity. *Macromolecules* **2013**, *46*, 5657−5663.
(27) Morfa, A. J.; Barnes, T. M.; Ferguson, A. J.; Levi, D. H.; Rumbles, G.; Rowlen, K. L.; van de Lagemaat, J. Optical Characterization of Pristine Poly(3-hexyl Thiophene) Films. *J. Polym. Sci., Part B: Polym. Phys.* **2011**, *49*, 186−194.
(28) Adachi, T.; Lakhwani, G.; Traub, M. C.; Ono, R. J.; Bielawski, C. W.; Barbara, P. F.; Vanden Bout, D. A. Conformational Effect on Energy Transfer in Single Polythiophene Chains. *J. Phys. Chem. B* **2012**, *116*, 9866−9872.
(29) Steiner, F.; Lupton, J. M.; Vogelsang, J. Role of Triplet-State Shelving in Organic Photovoltaics: Single-Chain Aggregates of Poly(3-Hexylthiophene) versus Mesoscopic Multichain Aggregates. *J. Am. Chem. Soc.* **2017**, *139*, 9787−9790.
(30) Ostrowski, D. P.; Lytwak, L. A.; Mejia, M. L.; Stevenson, K. J.; Holliday, B. J.; Vanden Bout, D. A. The Effects of Aggregation on Electronic and Optical Properties of Oligothiophene Particles. *ACS Nano* **2012**, *6*, 5507−5513.
(31) Hu, Z.; Willard, A. P.; Ono, R. J.; Bielawski, C. W.; Rossky, P. J.; Bout, D. A. V. An Insight into Non-Emissive Excited States in Conjugated Polymers. *Nat. Commun.* **2015**, *6*, 8246.
(32) Ho, P. K. H.; Kim, J.-S.; Tessler, N.; Friend, R. H. Photoluminescence of Poly(p-Phenylenevinylene)−Silica Nanocomposites: Evidence for Dual Emission by Franck−Condon Analysis. *J. Chem. Phys.* **2001**, *115*, 2709−2720.
(33) Paquin, F.; Yamagata, H.; Hestand, N. J.; Sakowicz, M.; Bérubé, N.; Côté, M.; Reynolds, L. X.; Haque, S. A.; Stingelin, N.; Spano, F. C.; Silva, C. Two-Dimensional Spatial Coherence of Excitons in Semicrystalline Polymeric Semiconductors: Effect of Molecular Weight. *Phys. Rev. B: Condens. Matter Mater. Phys.* **2013**, *88*, 155202.
(34) Scharsich, C.; Lohwasser, R. H.; Sommer, M.; Asawapirom, U.; Scherf, U.; Thelakkat, M.; Neher, D.; Köhler, A. Control of Aggregate Formation in Poly(3-Hexylthiophene) by Solvent, Molecular Weight, and Synthetic Method. *J. Polym. Sci., Part B: Polym. Phys.* **2012**, *50*, 442−453.
(35) Ferreira, B.; da Silva, P. F.; Seixas de Melo, J. S.; Pina, J.; Maçanita, A. Excited-State Dynamics and Self-Organization of Poly(3-Hexylthiophene) (P3HT) in Solution and Thin Films. *J. Phys. Chem. B* **2012**, *116*, 2347−2355.
(36) Johnson, C. E.; Boucher, D. S. Poly(3-Hexylthiophene) Aggregate Formation in Binary Solvent Mixtures: An Excitonic Coupling Analysis. *J. Polym. Sci., Part B: Polym. Phys.* **2014**, *52*, 526−538.
(37) van den Bogaart, G.; Kusters, I.; Velásquez, J.; Mika, J. T.; Krasnikov, V.; Driessen, A. J. M.; Poolman, B. Dual-Color Fluorescence-Burst Analysis to Study Pore Formation and Protein−Protein Interactions. *Methods* **2008**, *46*, 123−130.
(38) Schaaf, M. J. M.; Koopmans, W. J. A.; Meckel, T.; van Noort, J.; Snaar-Jagalska, B. E.; Schmidt, T. S.; Spaink, H. P. Single-Molecule Microscopy Reveals Membrane Microdomain Organization of Cells in a Living Vertebrate. *Biophys. J.* **2009**, *97*, 1206−1214.
(39) Baghgar, M.; Labastide, J.; Bokel, F.; Dujovne, I.; McKenna, A.; Barnes, A. M.; Pentzer, E.; Emrick, T.; Hayward, R.; Barnes, M. D. Probing Inter- and Intrachain Exciton Coupling in Isolated Poly(3-Hexylthiophene) Nanofibers: Effect of Solvation and Regioregularity. *J. Phys. Chem. Lett.* **2012**, *3*, 1674−1679.
(40) Jelley, E. E. Spectral Absorption and Fluorescence of Dyes in the Molecular State. *Nature* **1936**, *138*, 1009−1010.
(41) Spano, F. C.; Mukamel, S. Superradiance in Molecular Aggregates. *J. Chem. Phys.* **1989**, *91*, 683−700.
(42) Fidder, H.; Knoester, J.; Wiersma, D. A. Superradiant Emission and Optical Dephasing in J-Aggregates. *Chem. Phys. Lett.* **1990**, *171*, 529−536.
(43) Parkinson, P.; Müller, C.; Stingelin, N.; Johnston, M. B.; Herz, L. M. Role of Ultrafast Torsional Relaxation in the Emission from Polythiophene Aggregates. *J. Phys. Chem. Lett.* **2010**, *1*, 2788−2792.
(44) Banerji, N.; Cowan, S.; Vauthey, E.; Heeger, A. J. Ultrafast Relaxation of the Poly(3-Hexylthiophene) Emission Spectrum. *J. Phys. Chem. C* **2011**, *115*, 9726−9739.
(45) Lin, H.; Tian, Y.; Zapadka, K.; Persson, G.; Thomsson, D.; Mirzov, O.; Larsson, P.-O.; Widengren, J.; Scheblykin, I. G. Fate of Excitations in Conjugated Polymers: Single-Molecule Spectroscopy Reveals Nonemissive "Dark" Regions in MEH-PPV Individual Chains. *Nano Lett.* **2009**, *9*, 4456−4461.
(46) Cook, S.; Furube, A.; Katoh, R. Analysis of the Excited States of Regioregular Polythiophene P3HT. *Energy Environ. Sci.* **2008**, *1*, 294−299.
(47) Hou, L.; Adhikari, S.; Tian, Y.; Scheblykin, I. G.; Orrit, M. Absorption and Quantum Yield of Single Conjugated Polymer Poly[2-Methoxy-5-(2-Ethylhexyloxy)-1,4-Phenylenevinylene] (MEH-PPV) Molecules. *Nano Lett.* **2017**, *17*, 1575−1581.

https://doi.org/10.1021/acs.jpclett.1c01334
J. Phys. Chem. Lett. 2021, 12, 5919−5924